BIOCHEMISTRY
including biophysical chemistry & molecular biology

Article

pubs.acs.org/biochemistry

Structural and Biochemical Consequences of Disease-Causing Mutations in the Ankyrin Repeat Domain of the Human TRPV4 Channel

Hitoshi Inada,[†] Erik Procko,[†,‡] Marcos Sotomayor,[†,‡] and Rachelle Gaudet*[,†]

[†]Department of Molecular and Cellular Biology, Harvard University, 52 Oxford Street, Cambridge, Massachusetts 02138, United States

[‡]Howard Hughes Medical Institute and Department of Neurobiology, Harvard Medical School, Boston, Massachusetts 02115, United States

Supporting Information

ABSTRACT: The TRPV4 calcium-permeable cation channel plays important physiological roles in osmosensation, mechanosensation, cell barrier formation, and bone homeostasis. Recent studies reported that mutations in TRPV4, including some in its ankyrin repeat domain (ARD), are associated with human inherited diseases, including neuropathies and skeletal dysplasias, probably because of the increased constitutive activity of the channel. TRPV4 activity is regulated by the binding of calmodulin and small molecules such as ATP to the ARD at its cytoplasmic N-terminus. We determined structures of ATP-free and -bound forms of human TRPV4-ARD and compared them with available TRPV-ARD structures. The third inter-repeat loop region (Finger 3 loop) is flexible and may act as a switch to regulate channel activity. Comparisons of TRPV-ARD structures also suggest an evolutionary link between ARD structure and ATP binding ability. Thermal stability analyses and molecular dynamics simulations suggest that ATP increases stability in TRPV-ARDs that can bind ATP. Biochemical analyses of a large panel of TRPV4-ARD mutations associated with human inherited diseases showed that some impaired thermal stability while others weakened ATP binding ability, suggesting molecular mechanisms for the diseases.

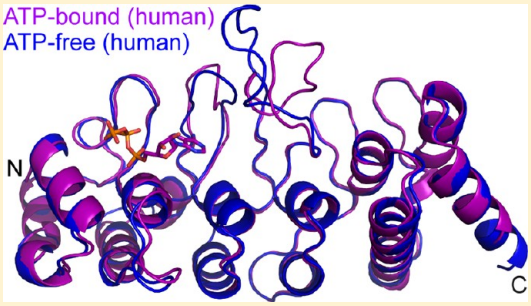

Transient receptor potential (TRP) channels are cation channels involved in sensation of various stimuli from internal and external environments. The TRP channel superfamily is divided into six subfamilies in mammals: canonical or classical TRPC, vanilloid TRPV, melastatin TRPM, ankyrin TRPA, mucolipin TRPML, and polycystin TRPP.[1−3] Six TRPV proteins, TRPV1−6, belong to the vanilloid subfamily. TRPV proteins function as tetramers, and each protomer contains six transmembrane segments flanked by two intracellular domains: a large N-terminal domain containing ankyrin repeats and a short C-terminal domain.

TRPV channel activity is regulated by post-translational modifications such as phosphorylation or binding of regulatory molecules to intracellular domains.[4,5] In TRPV1, for example, ATP and calmodulin (CaM) have been shown to bind to the N-terminal ankyrin repeat domain (ARD) and sensitize and desensitize channel activity, respectively.[6,7] The binding of ATP and CaM to the ARD is also conserved in TRPV4 and TRPV3.[8] Phosphatidylinositol 4,5-bisphosphate (PIP_2) and CaM interact with the C-terminal domain of TRPV1 and regulate channel activity.[9−11] The molecular mechanisms by which these intracellular signals regulate TRPV channel activity remain unclear.

TRPV4 is a member of the TRPV subfamily expressed broadly in neuronal and non-neuronal cells. TRPV4 is activated by various stimuli, including hypo-osmolarity, warm temperature, and chemical ligands such as 4-α-phorbol esters and epoxyeicosatrienoic acids.[12−15] Consistent with these in vitro findings, TRPV4 has been implicated in physiological functions such as osmoregulation and thermoregulation.[16,17] TRPV4 also plays a role in mechanosensation in the vascular endothelium and unitary tract,[18] and cell barrier formation in vascular and epidermal tissues.[19] Recently, studies using TRPV4 knockout mice suggested the functional importance of TRPV4 in the central nervous system, nociception, and bone formation.[20−22]

Mutations in TRPV4 are associated with a wide spectrum of inherited diseases, primarily autosomal dominant neuropathies and skeletal dysplasias.[23,24] Several mutants studied in heterologous expression systems showed constitutive basal activity and enhanced response to stimuli.[25−28] These findings are consistent with cell death caused by high calcium influx such as the observed degeneration of motor neurons in neuropathies.[27,28] However, it is difficult to explain how seemingly similar molecular properties lead to such diverse disease phenotypes. It is therefore essential to elucidate how

Received: February 28, 2012
Revised: May 27, 2012
Published: June 15, 2012

dx.doi.org/10.1021/bi300279b | *Biochemistry* 2012, 51, 6195−6206

TRPV4 is regulated at the molecular level to understand the mechanisms behind these inherited diseases.

To obtain insight into regulatory mechanisms of TRPV4, we focused on TRPV4-ARD, which can mediate channel regulation through binding of ligands to its concave surface and is the target of many mutations causing human diseases. We determined the structures of ATP-free and -bound human TRPV4-ARD and compared them with the structures of the other TRPV-ARDs. Despite a number of TRPV-ARD structures available in the absence or presence of ATP, this represents the first cognate pair of ATP-free and -bound structures. Structural analysis revealed that a long loop forming Finger 3 is flexible and could switch conformation to possibly regulate channel activity. Comparisons of TRPV-ARD structures provide further insights into the evolution of ATP binding in TRPV channels. Thermal stability analyses, a cysteine accessibility assay, and molecular dynamics (MD) simulations indicate that ATP binding can stabilize TRPV1- and TRPV4-ARD. Interestingly, most mutations causing human genetic diseases in TRPV4-ARD are located away from the ATP-binding site, suggesting that additional regulatory interactions and mechanisms exist. A series of biochemical analyses of disease-associated mutants showed that some impaired thermal stability and/or ATP binding ability, providing biochemical insights into possible disease mechanisms.

EXPERIMENTAL PROCEDURES

Expression Constructs. Human TRPV4 cDNA was obtained from C. J. Sumner. The DNA fragment corresponding to the ARD (residues 149−396) was amplified by polymerase chain reaction and subcloned into the NdeI and NotI sites of a pET vector with a C-terminal six-histidine tag (pET21-C6H).[29] Mutations were generated with QuikChange (Stratagene) and confirmed by DNA sequencing.

Protein Production and Purification. Recombinant human TRPV4-ARD protein was expressed in *Escherichia coli* BL21(DE3) by induction with 75 μM isopropyl β-D-thiogalactopyranoside for 13 h at room temperature after the cells reached an OD_{600} of ∼0.6. Frozen cell pellets were thawed, resuspended, and lysed by sonication in lysis buffer [20 mM Tris-HCl, 300 mM NaCl, and 20 mM imidazole (pH 7.0)] with 1 mM benzamidine, 1 mM phenylmethanesulfonyl fluoride (PMSF), 0.1% Triton X-100, 0.2 mg/mL lysozyme, 50 μg/mL RNase A, and 25 μg/mL DNase I. The lysate was cleared by centrifugation and the supernatant loaded onto nickel-nitrilotriacetic acid (Ni-NTA) agarose (Qiagen) and eluted with a step gradient containing 25, 50, 100, 150, 200, and 250 mM imidazole (pH 7.0) in lysis buffer with 0.05% β-mercaptoethanol and 0.5 mM PMSF. Fractions containing the protein at 150, 200, and 250 mM imidazole were combined, and EDTA (pH 8.0) was added to a final concentration of 1 mM and then the mixture dialyzed against 20 mM Tris-HCl (pH 7.0), 50 mM NaCl, 1 mM EDTA, and 1 mM DTT. The dialyzed protein was purified on SP Sepharose FF (GE Healthcare, Piscataway, NJ) in 20 mM Tris-HCl (pH 7.0), 1 mM EDTA, and 1 mM DTT using a linear gradient from 0 to 0.4 M NaCl. Size exclusion chromatography on a Superdex 75 column (GE Healthcare) in 10 mM Tris-HCl (pH 7.0), 300 mM NaCl, 10% glycerol, and 1 mM DTT was used for final purification. Protein was concentrated to ∼8 mg/mL in a Vivaspin centrifugal filter (10000 molecular weight cutoff; Sartorius AG, Goettingen, Germany), flash-frozen, and stored at −80 °C. In the purification of mutant proteins for the thermal stability assay, dialysis and ion exchange steps were omitted. After Ni-NTA purification, the proteins were purified by size exclusion chromatography in phosphate-buffered saline (pH 7.4) with 1 mM DTT. Rat TRPV1-ARD (rTRPV1-ARD) was purified as described previously.[7]

Crystallization of Human TRPV4-ARD. Crystals were grown by hanging-drop vapor diffusion at 4 °C: the ATP-free form with a 1:3 ratio of protein to reservoir solution [0.35 M NaH_2PO_4, 0.35 M KH_2PO_4, 10% glycerol, and 0.1 M Na-HEPES (pH 7.8)] and the ATP-bound form with a 1:1 ratio of protein to reservoir [3% PEG 4000, 10% glycerol, and 0.1 M Na-HEPES (pH 7.9)] in the presence of 5 mM ATP. Crystals were soaked in reservoir solution containing 15% glucose for 3 min, transferred into reservoir solution containing 30% glucose, and flash-frozen in liquid nitrogen.

Data Collection, Structure Determination, and Analysis. X-ray data were collected at 100 K using an ADSC Q315 detector at the Advanced Photon Source ID24 beamline, processed in HKL2000;[30] data statistics are listed in Table 1. The hTRPV4-ARD structures were determined by molecular replacement using the chicken TRPV4-ARD structure in MOLREP[31] and Phaser.[32] Model building was performed in COOT[33] and refinement with TLS (Translation/Libration/Screw) in REFMAC5.[34] Final refinement statistics are listed in Table 1. The coordinates have been deposited in the Protein Data Bank (PDB) as entries 4DX1 (ATP-free) and 4DX2 (ATP-bound). Figures were generated with PyMOL (Schrödinger, LLC).

Thermal Stability Assay by Circular Dichroism Spectroscopy. Circular dichroism (CD) spectra were measured at 10 °C with 3.4 μM protein in 150 mM NaCl, 5 mM Tris-HCl (pH 7.5), and 1 mM DTT for experiments testing the influence of ATP on protein stability, and in phosphate-buffered saline (pH 7.4) with 1 mM DTT for analyses of the wild type and mutants. CD spectra were recorded in a 1 mm path length cuvette on a Jasco J-815 spectropolarimeter. For thermal stability, the molar ellipticity at λ = 222 nm was measured as the protein solutions were heated at a rate of 1 °C/min and used to determine the fraction of protein folded (assuming a completely folded protein population at a starting temperature of 10 °C). Thermal denaturation temperatures (T_m) were analyzed with Jasco Spectra software (JASCO Inc., Easton, MD) and are given with their standard deviation (SD).

Molecular Dynamics Simulation of rTRPV1-ARD. Two sets of molecular dynamics simulations (apo and ATP) were conducted using the structure of rTRPV1-ARD bound to ATP, with and without the ATP ligand removed in silico, respectively (PDB entry 2PNN, residues 111−356). Structures were solvated in explicit water (TIP3) and ions (100 mM NaCl) using VMD.[35] The systems contained 208501 (ATP) and 208482 (apo) atoms. Minimization, equilibration, and steered molecular dynamics (SMD) simulations were performed in multiple steps using NAMD2.7,[36] the CHARMM27 force field for proteins with the CMAP correction,[37,38] full electrostatics, and 2 fs time steps with hydrogen bonds constrained. SMD simulations stretched both ends of TRPV1-ARD at effective speeds of 2 and 20 nm/ns.

ATP-Agarose Pull-Down Assays. The ATP-agarose assays were performed as described previously.[28] Briefly, 20 μg of protein was incubated with 70 or 75 μL of a 50% ATP agarose slurry for 1 h at 4 °C in binding buffer [10 mM Tris-HCl (pH 7.0), 50 mM NaCl, 1 mM DTT, and 0.15% *n*-decyl D-

dx.doi.org/10.1021/bi300279b | *Biochemistry* 2012, 51, 6195−6206

Table 1. Data Collection and Refinement Statistics

	crystal form I (ATP-free)	crystal form II (with ATP)
	Data Collection	
space group	$P3_121$	$P3_221$
wavelength (Å)	0.97917	0.97917
cell dimensions *a*, *b*, *c* (Å)	53.30, 53.37, 440.71	147.89, 147.89, 93.90
resolution (Å)[a]	40.0−2.85 (2.90−2.85)	40.0−2.95 (3.00−2.95)
R_{sym}[a]	0.115 (0.614)	0.099 (0.714)
$I/\sigma(I)$[a]	12.3 (1.8)	17.6 (2.4)
completeness (%)[a]	99.6 (99.3)	100.0 (100.0)
redundancy[a]	5.3. (5.4)	5.5 (5.6)
	Refinement	
resolution (Å)[a]	39.2−2.85 (2.92−2.85)	38.86−2.95 (3.03−2.95)
no. of reflections	17306	23958
R_{work}/R_{free}	0.215/0.278	0.177/0.220
no. of molecules per asymmetric unit	2	2
no. of residues in model	148−397 (chain A)	148−394 (ATP-bound)
	148−396 (chain B)	148−392 (ATP-unbound)
no. of atoms		
protein	1995 (chain A)	1987 (ATP-bound)
	1986 (chain B)	1963 (ATP-unbound)
ligand	25 (PO_4)	31 (ATP)
	6 (glycerol)	6 (glycerol)
		12 (glucose)
water	18	72
B factor (Å)		
protein	80.91	62.12 (ATP-bound)
		72.76 (ATP-unbound)
ligand	113.98 (PO_4)	91.00 (ATP)
	103.44 (glycerol)	72.51 (glycerol)
		90.86 (glucose)
water	76.06	54.84
rmsd		
bond lengths (Å)	0.013	0.013
bond angles (deg)	1.51	1.80

[a]Values from the highest-resolution shell are in parentheses.

maltopyranoside]. After the agarose had been washed three times, proteins were extracted and loaded onto the 15% SDS gel. In each load lane, the volumes loaded corresponded to 1 μg of protein. Gels were quantified using ImageJ (National Institutes of Health, Bethesda, MD), and shown are the averages ± SD for three independent experiments.

TRPV1 Cysteine Modification Assay. Reaction mixtures containing rTRPV1-ARD (8.5 μM) in 150 mM NaCl, 20 mM Tris (pH 7.0), 0.5 mM PEG-maleimide 5 kDa (Creative PEGWorks), and 10 mM nucleotide as indicated were incubated at room temperature, reactions stopped by addition of DTT to a final concentration of 110 mM, and mixtures analyzed by Coomassie-stained 12% SDS−PAGE.

Statistical Analyses. Statistical significance was tested by multiple comparisons using Tukey-Kramer or Dunnett's method with JMP software (SAS Institute Inc., Cary, NC).

RESULTS

Structures of Human TRPV4-ARD. Recombinant human TRPV4-ARD (hTRPV4-ARD, residues 149−396) produced in *E. coli* was purified for structure determination by X-ray crystallography and biochemical analyses. We determined the structure of hTRPV4-ARD in the absence (crystal form I, ATP-free) or presence (crystal form II) of ATP (Table 1). Both crystal forms contain two molecules per asymmetric unit. In crystal form II, one molecule is bound to ATP (ATP-bound) while the other is not (ATP-unbound). As expected on the basis of previous structures of TRPV-ARDs,[7] hTRPV4-ARD consists of six ankyrin repeats (ANK1−6) each containing an inner and an outer helix followed by a connecting finger loop (Fingers 1−5) (Figure 1A). The inner helices and fingers form

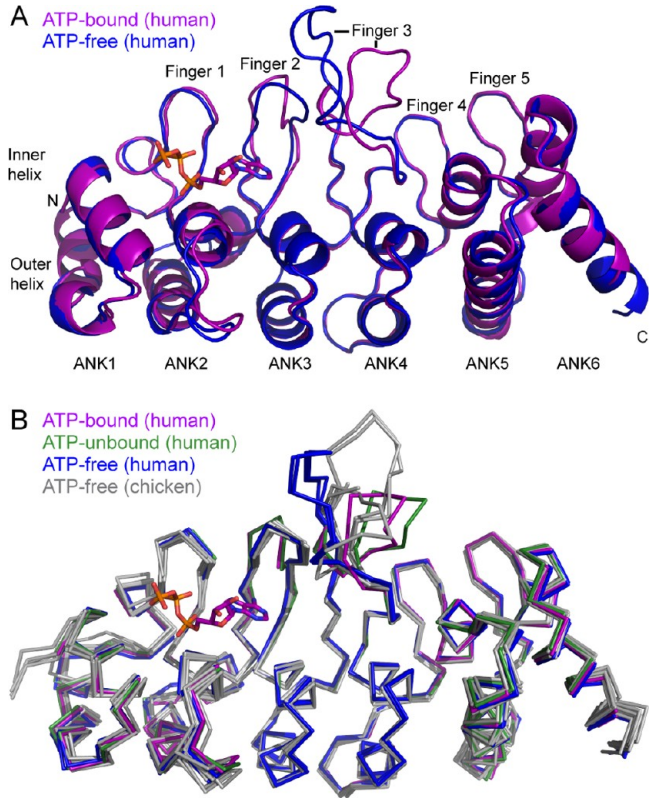

Figure 1. Structural comparison of human and chicken TRPV4-ARDs. (A) Superimposed ribbon diagrams of ATP-bound (magenta) and ATP-free (blue) hTRPV4-ARD. ATP is shown as sticks. (B) Superimposed Cα traces of human and chicken TRPV4-ARD. Finger 3 is twisted and shrunken in the ATP-bound (magenta) and ATP-unbound (green) hTRPV4-ARD structures, while the finger is extended in ATP-free hTRPV4-ARD (blue) and cTRPV4-ARD (gray). Several Finger 3 residues are disordered in three of six TRPV4-ARD structures. The structure of Finger 2 in the ATP-bound and -unbound forms differs from that in ATP-free forms.

a concave surface to which ATP is bound at the expected site previously identified in TRPV1.[7] Importantly, these structures represent the first cognate pair of ATP-bound and ATP-free TRPV-ARD structures.

The structures of hTRPV4-ARD were compared to each other and to those of chicken TRPV4-ARD (cTRPV4-ARD).[28] The structures of ATP-free hTRPV4-ARD and cTRPV4-ARD (residues 133−382, 90% identical sequences) are very similar (rmsd ranges from 0.635 to 0.922 Å over 239−242 Cα atoms)

dx.doi.org/10.1021/bi300279b | *Biochemistry* 2012, 51, 6195−6206

except at the tips of Fingers 2 and 3 (Figure 1B). The same trend is apparent when extending this comparison to all 10 available structures of TRPV4-ARD (four hTRPV4-ARD molecules in two crystal forms and six cTRPV4-ARD molecules in two crystal forms as well), with large structural differences observed in the very long Finger 3, as well as in the tip of Finger 2. Consistently, Finger 3 residues had high *B* factors and were too disordered to trace in several cTRPV4-ARD structures, indicating high flexibility.

Structural Consequences of ATP Binding. Direct comparisons of the ATP-free and ATP-bound hTRPV4-ARD structures again show conformational differences restricted to Fingers 2 and 3 (Figure 1A). Finger 3 was extended in ATP-free hTRPV4-ARD (and in ATP-free cTRPV4-ARD), while the finger loop was twisted and shrunken in ATP-bound hTRPV4-ARD. Finger 2 was also slightly twisted in ATP-bound hTRPV4-ARD. Surprisingly, both conformational differences were also observed when comparing the second, ATP-unbound, molecule in crystal form II to the ATP-free crystal form I structures (Figure 1B). In crystal form II, an adjacent symmetry-related hTRPV4-ARD molecule occupied the ATP-binding site of the ATP-unbound molecule, possibly mimicking ATP binding. Alternatively, the shrunken Finger 3 structure may result from crystal contacts and/or crystallization condition differences.

One unusual feature of TRPV-ARDs is that many aromatic residues are exposed on flexible Fingers 2 and 3.[29] In hTRPV4-ARD, 9 of 20 aromatic residues are located on the concave face of Fingers 2 and 3 [three and six residues, respectively (Figure 2)]. Interestingly, F272 and F273 on Finger 3 are exposed in the ATP-free form, while these phenylalanines are buried in the shrunken Finger 3 of the ATP-bound form (Figure 2B). The observed conformational differences may thus serve to regulate the exposure of the aromatic patch, and the conservation of the patch suggests that it is important, perhaps in interactions with regulatory ligands or with other regions of the full TRPV4 homotetramer.

Structural Comparison of TRPV-ARDs. Multiple TRPV-ARD structures are available: a structure of rat TRPV1-ARD (rTRPV1-ARD) bound to ATP,[7] structures of cTRPV4-ARD in the absence of ATP, and structures of several ARDs that do not bind ATP, namely, rat and human TRPV2-ARDs and mouse TRPV6-ARD[28,39,40] (see Table S1 of the Supporting Information). The overall structures of all available TRPV-ARDs are similar, with rmsd values ranging from 0.637 to 1.865 Å over 139−155 core Cα atoms (Table S2 of the Supporting Information). A superposition of all structures illustrates that the largest structural differences are again found in Fingers 2 and 3 (Figure 3A). Structural comparisons of these TRPV-ARDs and the new human TRPV4-ARD highlight three noteworthy features.

First, as expected from biochemical, mutational, and sequence analyses,[8] the interaction of ATP with hTRPV4-ARD is very similar to what was previously observed in rTRPV1-ARD (Figure 3B).[7] The adenine base fits in a conserved pocket, stacking against Tyr236 and hydrogen bonding to Gln239. Furthermore, Lys192 and Lys197 on the surface of inner helix 2 interact with the phosphate groups of ATP. These lysines are homologous to lysines critical for ATP binding in rTRPV1-ARD (Lys155 and Lys160)[7] and cTRPV4-ARD (Lys178 and Lys183).[8] The importance of Lys197 in ATP binding is further discussed below. The γ-phosphate of the ATP is further removed from the protein in TRPV4 compared to

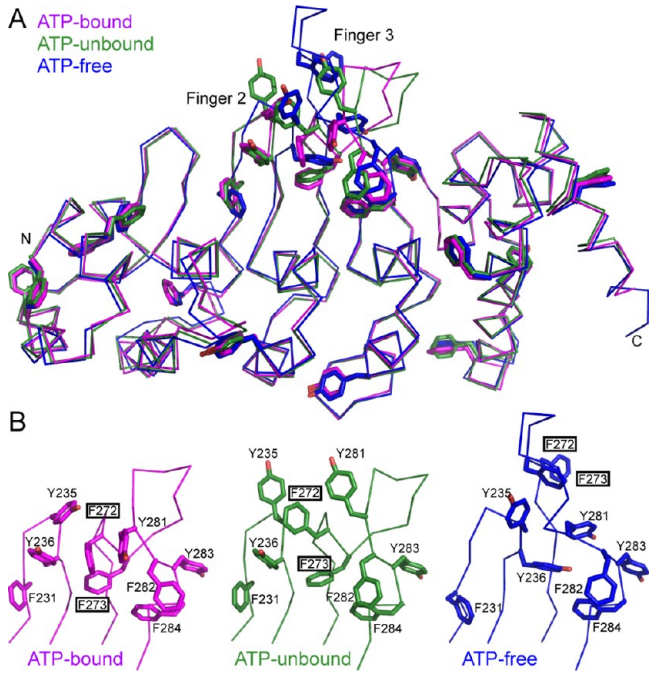

Figure 2. Aromatic residues on Fingers 2 and 3 have varied positions in hTRPV4-ARD structures. (A) The hTRPV4-ARD structures of ATP-bound (magenta), ATP-unbound (green), and ATP-free (blue) forms are superimposed. Aromatic residues are shown as sticks. (B) Detail of the Finger 2 and 3 loops. F272 and F273 on Finger 3 (black rectangles) are embedded in the aromatic cluster in the ATP-bound and -unbound forms but exposed in the ATP-free form. Y235 and Y236 on Finger 2 and Y281 and F282 on Finger 3 are located in similar positions but show variable orientations. F231, F282, Y283, and F284 show less variation.

TRPV1, consistent with the fact that TRPV4-ARD exhibited less selectivity for ATP over ADP in ATP-agarose competition assays.[7]

Second, the backbone structure of ATP-bound hTRPV4-ARD, with a collapsed Finger 3, is quite similar to those of TRPV2-ARD and TRPV6-ARD, which lack the ability to bind ATP (Figure 3C). In contrast, the ATP-free structures of chicken and human TRPV4-ARD, which both have the ability to bind ATP, have extended Finger 3 conformations (Figures 1B and 3A). This visual observation is supported by a comparison of rmsd values for Fingers 2 and 3 of both ATP-free and -bound forms of hTRPV4-ARD with TRPV2-ARDs and mTRPV6-ARD: the ATP-bound form generally showed smaller rmsds than the ATP-free form (Table S2 of the Supporting Information). This suggests that although the ARDs of TRPV2 and TRPV6 do not bind ATP, they are closest to the ATP-bound state of ARDs with ATP-binding sites, at least in structural terms.

Finally, the structure of ATP-bound hTRPV4-ARD and comparisons to TRPV2 and TRPV6 suggest that a previously unrecognized residue, Phe231 in hTRPV4-ARD, could be important for ATP binding. Phe231 is located under the adenine-stacking Tyr236 on Finger 2 (Figure 3D), contributing to the adenine-binding pocket. This aromatic residue is conserved in the ATP-binding site of rTRPV1-ARD (Tyr194), while the aromatic residues are substituted with a smaller aliphatic residue, cysteine or methionine, in TRPV2 or TRPV6, respectively (Figure 3E). Sequence alignments of TRPV proteins confirm this trend, as the equivalent residue is a

dx.doi.org/10.1021/bi300279b | *Biochemistry* 2012, 51, 6195−6206

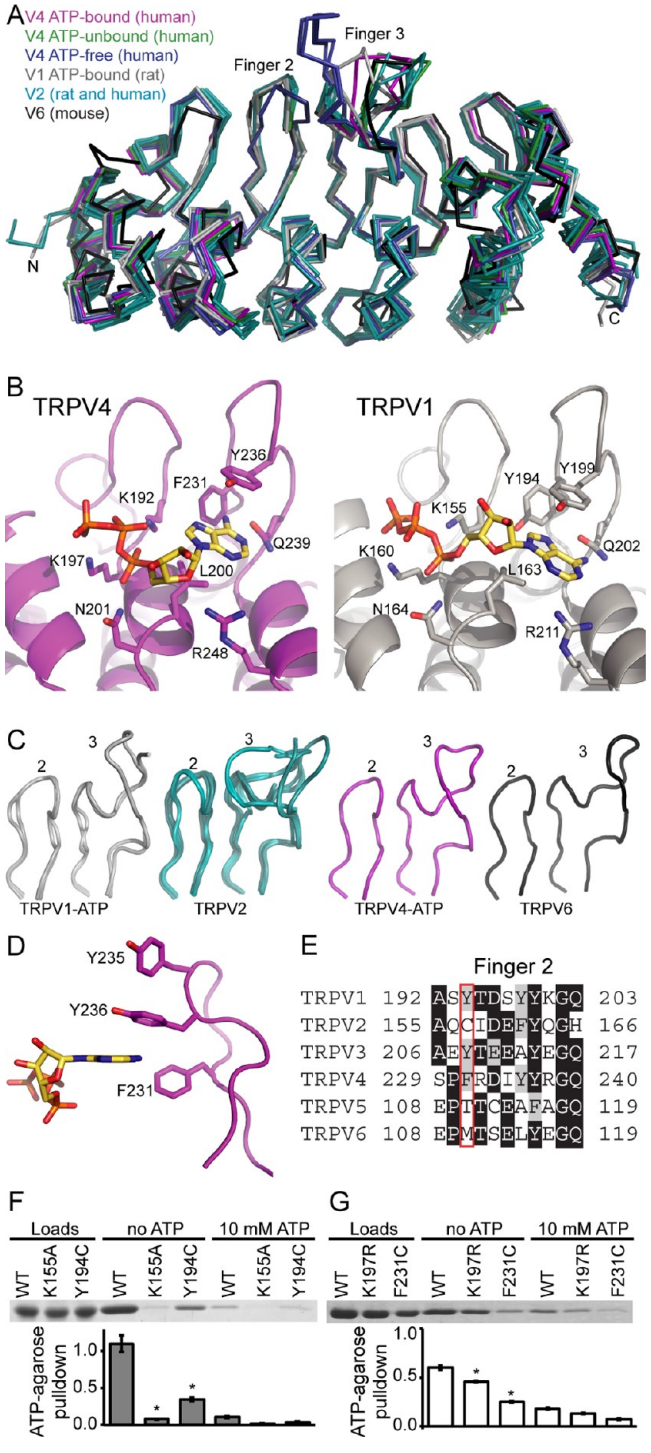

Figure 3. Structural comparison of TRPV-ARDs. (A) Superimposed main chain structure of TRPV-ARDs (rTRPV1-ARD, gray; rat and human TRPV2-ARD, cyan; ATP-bound hTRPV4-ARD, magenta; ATP-unbound hTRPV4-ARD, green; ATP-free hTRPV4-ARD, blue; and mouse TRPV6-ARD, black). Finger 3 and a part of Finger 2 are highly flexible. Several residues on Finger 3 are missing in one of two TRPV1-ARD structures and four of seven TRPV2-ARD structures. (B) ATP-binding site of hTRPV4-ARD and rTRPV1-ARD. Residues (sticks) within 4 Å of the ATP molecule and a surface map of the ATP-binding site in hTRPV4-ARD (left) and the corresponding residues in the rTRPV1-ARD ATP-binding site (right). The bBound ATP molecule is shown as sticks (orange and yellow). (C) Finger 2 (2) and Finger 3 (3) structures of ATP-bound rat TRPV1-ARD (gray), rat and human TRPV2-ARD (cyan), human ATP-bound TRPV4-ARD (magenta), and mouse TRPV6-ARD (black). (D) Aromatic residue positioned behind the adenine base of ATP in Finger 2 (F231 in human TRPV4-ARD). (E) This aromatic residue is conserved in TRPV-ARDs that bind ATP (red rectangle). (F and G) ATP-agarose pull-down assays for wild-type and mutant rTRPV1-ARD (F) or hTRPV4-ARD (G). Coomassie-stained gels (top) of wild-type and mutant proteins loaded (left) and bound to ATP-agarose in the absence (middle) or presence (right) of competing free ATP. The normalized intensity of protein recovered (mean ± SD; n = 3) is plotted below. The statistical significance of the change in binding to ATP-agarose with respect to the wild type (WT) was determined by a multiple-comparison test using Dunnett's method, with $p < 0.01$ indicated by an asterisk.

tyrosine in TRPV3, which binds ATP, and threonine in TRPV5, which does not. Substitution of these aromatic residues with cysteine (the residue found in the equivalent position in TRPV2) caused a significant reduction in the level of ATP binding in both rTRPV1-ARD and hTRPV4-ARD. In rTRPV1-ARD, the Y194C mutation reduced the level of ATP binding comparably to the K155A mutation identified in a previous study (Figure 3F).[7] A significant reduction in the level of ATP binding was also observed in hTRPV4-ARD mutant F231C (Figure 3G). These results indicate that the buried aromatic residue in Finger 2 conserved in TRPV1, TRPV3, and TRPV4 does indeed contribute to ATP binding in rTRPV1-ARD and hTRPV4-ARD.

ATP Binding Stabilizes TRPV4-ARD and TRPV1-ARD. ATP binding does not result in large conformational changes, but the ATP-bound form showed a tightly packed Finger 3 in both rTRPV1-ARD and hTRPV4-ARD structures, leading us to hypothesize that ATP may stabilize the proteins. In other ankyrin repeat proteins, such as IκBα and Notch, the ankyrin repeats are partially folded and complete their folding as a ligand is bound.[41−43] We therefore sought to determine whether ATP binding affected ARD stability. To this end, we analyzed the thermal stability of hTRPV4-ARD by CD spectroscopy in the absence or presence of ATP, AMP, or phosphate (Figure 4). In buffer alone, hTRPV4-ARD showed a melting temperature (T_m) of 37.1 ± 0.1 °C. Phosphate ions (1 mM) increased T_m slightly but not significantly (37.33 ± 0.07 °C). In the presence of nucleotide ligands (1 mM), however, a small but significant increase in T_m was observed (T_m = 37.9 ± 0.2 °C for ATP and 37.4 ± 0.2 for AMP). The greater stabilization observed with ATP compared to AMP matches their differing binding affinity observed with cTRPV4-ARD.[8]

Stabilization of the ARD fold by nucleotides may also affect the accessibility of buried cysteine residues. hTRPV4-ARD contains four cysteines, two exposed (Cys194 and Cys250) and two buried (Cys294 and Cys353; Figure S1 of the Supporting Information). We examined the effect of ATP binding on ARD stability by measuring the kinetics of cysteine modification with PEG-maleimide (mPEG) in the presence or absence of 10 mM AMP or ATP. hTRPV4-ARD was modified at endogenous cysteines by a 5 kDa PEG-maleimide, resulting in multiple shifted bands on SDS−PAGE. Furthermore, the rate of protein modification with mPEG was significantly reduced in the presence of nucleotides, especially ATP (Figure S1 of the Supporting Information). This suggests that the ARD fold is quite flexible, and that ATP binding stabilizes the fold, consistent with the thermal stability results described above.

dx.doi.org/10.1021/bi300279b | Biochemistry 2012, 51, 6195−6206

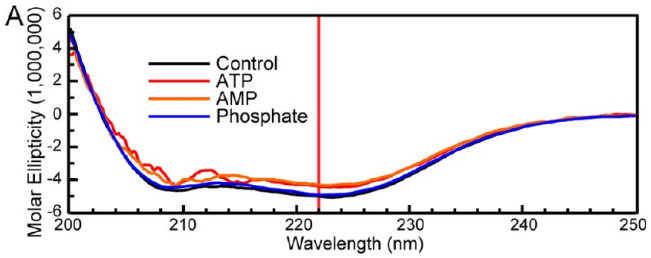

C

Condition	n	$T_m \pm SD$ (°C)
Control	4	37.1 ± 0.1
ATP	4	37.9 ± 0.2
AMP	4	37.4 ± 0.2
PO_4	4	37.33 ± 0.07

Figure 4. Effect of ATP on hTRPV4-ARD thermal stability. (A) Representative circular dichroism spectra of the purified TRPV4-ARD protein (3.4 μM) in the presence of ATP, AMP, or phosphate (1 mM each) at 10 °C. The wavelength (λ) of 222 nm used for thermostability assays is indicated by a vertical red line. (B) Representative traces of the thermostability assay. The molar ellipticity at 222 nm was measured as the protein solutions were heated at a rate of 1 °C/min. (C) T_m of TRPV4-ARD in the presence of 1 mM ATP, AMP, or phosphate. The statistical significance of the change in T_m was determined by a multiple-comparison test using the Tukey–Kramer method, with $p < 0.05$ and $p < 0.01$ indicated by one asterisk and two asterisks, respectively.

To gain further insights into the effect of ATP binding on ARD stability, we used single-cysteine mutants, allowing us to specifically address the accessibility of a buried cysteine. Interestingly, rTRPV1-ARD possesses a cysteine residue accessible to chemical modification by allicin, the active compound in garlic extract.[44] This cysteine residue, Cys157 (corresponding to Cys194 in hTRPV4-ARD), is paradoxically buried within the hydrophobic core of TRPV1-ARD (Figure 5A), suggesting that the structure may have some flexibility in solution, similar to that hypothesized for TRPV4-ARD above. Indeed, rTRPV1-ARD was modified at endogenous cysteines, like hTRPV4-ARD, whereas no mobility shift was observed in a cysteine-less rTRPV1-ARD variant (CL) (Figure 5B). More importantly, PEG-maleimide modification of a single-cysteine variant (C157) of rTRPV1-ARD, in which all cysteines except Cys157 were substituted with serine (C126S/C257S/C362S), resulted in a single shifted band (Figure 5B). This result demonstrates that buried Cys157 is indeed accessible to modification (Figure 5B), indicating a flexible and/or unstable fold. We hypothesized that ATP binding may stabilize the rTRPV1-ARD fold as it did hTRPV4-ARD. To test this hypothesis biochemically, we took advantage of the modifiable property of Cys157 to test the accessibility of this residue in the presence or absence of ATP. The single-cysteine variant rTRPV1-ARD CL-TRPV1-ARD C157 was chemically modified by PEG-maleimide with a half-time of 4 min ($t_{1/2}$ = 4 min) at room temperature (Figure 5C,D). Incubation with 10 mM ATP greatly inhibited the reaction, with a $t_{1/2}$ of 52 min, consistent with ATP stabilizing rTRPV1-ARD and limiting access to buried Cys157. In contrast, incubation with 10 mM ADP, a poor rTRPV1-ARD ligand,[7] only weakly inhibited Cys157 modification ($t_{1/2}$ = 10 min). CL-TRPV1-ARD C362, containing a single surface-exposed cysteine in the disordered C-terminal tail of the rTRPV1-ARD construct, was rapidly modified ($t_{1/2}$ < 30 s) even in the presence of nucleotides, confirming that ATP specifically inhibits the reaction of buried Cys157 (Figure 5C,D). Therefore, as shown for hTRPV4-ARD above using CD spectroscopy, cysteine modification of hTRPV4-ARD and rTRPV1-ARD indicates that ATP binding can stabilize the TRPV-ARD fold.

To further confirm our results, we used steered molecular dynamics (SMD)[45] to pull the termini of TRPV1-ARD and reveal stable regions during protein mechanical unfolding in silico. The N- and C-termini were separated at a constant velocity of 2 or 20 nm/ns in the presence or absence of bound ATP. TRPV1-ARD simulated in the absence of bound ATP unfolded at both ends, with repeats 6 and then 1 unraveling during the time periods of independent simulations performed at either stretching speed (Figure 5E,F). In contrast, when ATP, bound to repeats 1–3, was included in the simulations, repeat 6 and much of repeat 5 unravelled, while repeat 1 remained essentially intact (Figure 5G,H). Unfolding forces were similar in the presence or absence of bound ATP at fast stretching speeds, but slightly larger for the ATP-bound ARD in the slower stretching simulations (Figure S2 of the Supporting Information). These simulations therefore support the idea that ATP stabilizes the surrounding local TRPV1-ARD structure. Dynamic ligand-induced changes in TRPV-ARD stability may therefore provide a regulatory mechanism for channel sensitivity and activation.

Structural Analysis of TRPV4 Mutations Associated with Human Diseases. Many mutations in the TRPV4 gene have been associated with inherited diseases.[23,24] Within the ARD, at least 15 mutations at 12 residues have been reported to cause autosomal dominant diseases classified as either neuropathies or skeletal dysplasias (Figure 6A).[46−48] Mutations at arginine residues located on the convex face of hTRPV4-ARD are associated with neuropathies (Figure 6B).[49] Arg232 and Arg269 are located on Fingers 2 and 3, respectively, while Arg315 and Arg316 are located at the base of Finger 4. In contrast, eight residues whose mutations are associated with skeletal dysplasias (Glu183, Lys197, Leu199, Glu278, Thr295, Ile331, Asp333, and Val342) are spread on both fingers and helices, primarily on the concave face of hTRPV4-ARD (Figure 2B). Therefore, mapping the available genetic data on the hTRPV4-ARD structure suggests that the phenotypic differences of the diseases may be related to the differing functional properties of the concave and convex ARD surfaces.

To gain insights into possible biochemical mechanisms connecting the mutations with disease phenotypes, we generated mutant hTRPV4-ARD corresponding to 13 of the 15 disease-causing mutations located within the ARD. We were not able to produce recombinant T295A hTRPV4-ARD because of its low level of protein expression and/or stability. The inability of T295A to fold stably when expressed in *E. coli* and the influence of nucleotide ligands on the thermal stability of hTRPV4-ARD suggest that several mutations could affect protein folding and/or stability. We therefore tested the

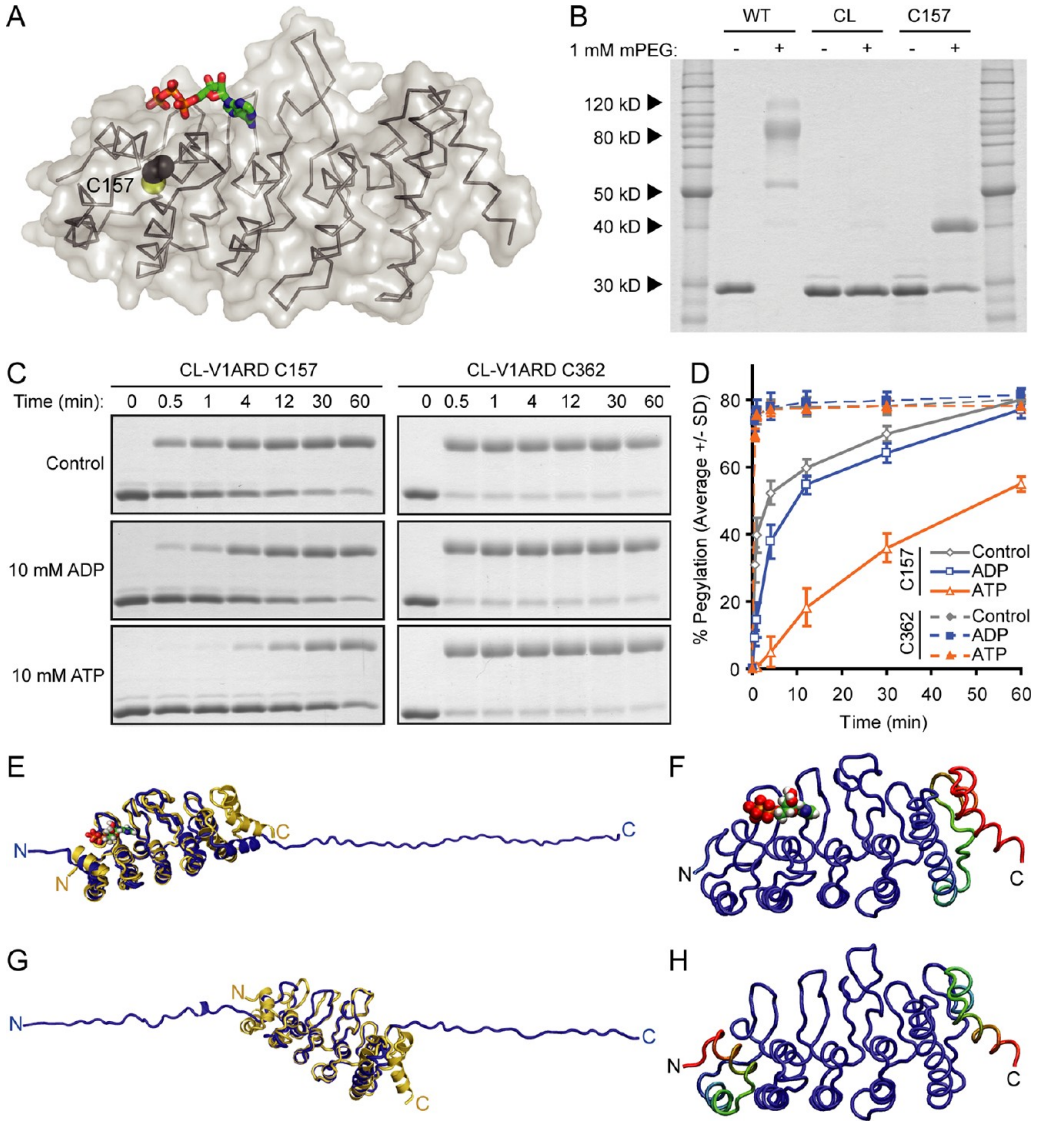

Figure 5. Effect of ATP binding on protein stability in rTRPV1-ARD. (A) Structure of TRPV1-ARD (gray) bound to ATP (green, sticks), with buried Cys157 highlighted (spheres). (B) TRPV1-ARD is modified at cysteine residues by PEG-maleimide (mPEG), causing an electrophoretic mobility shift on a Coomassie-stained SDS gel. Abbreviations: WT, wild type; CL, a cysteine-less variant; C157, CL-TRPV1-ARD C157 single-cysteine variant. Shown is a representative Coomassie-stained gel from one of three experiments. (C) Time course for modification of single-cysteine TRPV1-ARD variants C157 and C362 with 0.5 mM mPEG at room temperature. (D) Data from four experiments like that depicted in panel C were quantified, and the mean ± standard deviation was plotted. (E and F) Molecular dynamics simulation in which the termini of the ATP-bound TRPV1-ARD (E) or TRPV1-ARD structure with ATP removed prior to equilibrating the system (F) are pulled apart at a rate of 20 nm/ns. Superimposed are the structures at the start (gold) and end (blue) of the simulations. (G and H) Root-mean-square deviation of each Cα atom over the course of the simulation mapped onto the starting models with (G) or without (H) ATP. The change in color from blue to red indicates changes in rmsd from 0 to 80 Å. Simulations in which the termini were pulled apart at a rate of 2 nm/ns gave similar results. See Table S3 of the Supporting Information for experimental details.

thermal stability of wild-type hTRPV4-ARD and the 13 purified hTRPV4-ARD mutants by CD spectroscopy. Wild-type hTRPV4-ARD had a melting temperature (T_m) of 37.93 ± 0.08 °C (note that a phosphate-based buffer was used for these experiments). The T_m values of most mutants were significantly different from that of the wild type, except for those of R232C and I331T [38.1 ± 0.1 and 37.97 ± 0.07 °C, respectively (Table S4 and Figure S3 of the Supporting Information)]. Most mutations resulted in a significantly lower T_m values, although R269C showed a significantly higher T_m (38.6 ± 0.2 °C) than the wild type (Table S4 of the Supporting Information). L199F and E183K showed the more severe reductions in T_m (32.9 ± 0.1 and 33.78 ± 0.06 °C, respectively). Leu199 is buried and tightly packed between inner helices 2 and 3, and therefore, its substitution with a larger phenylalanine side chain likely affects the protein thermal stability by disrupting the hydrophobic core packing arrangement (Figure 6C). Glu183 is on the surface of Finger 2 and forms a salt bridge to Arg232 in some of the hTRPV4-ARD structures (Figure 6D). However, simple disruption of this salt bridge is unlikely to cause this decrease in stability because the complementary R232C neutralizing mutation did not significantly alter the T_m of hTRPV4-ARD. The E183K charge reversal may cause electrostatic repulsion between the ANK fingers due to the proximity of Arg232, while the R232C mutation, disrupting the salt bridge, would not actively cause electrostatic repulsion. Overall, the averaged T_m

dx.doi.org/10.1021/bi300279b | *Biochemistry* 2012, 51, 6195−6206

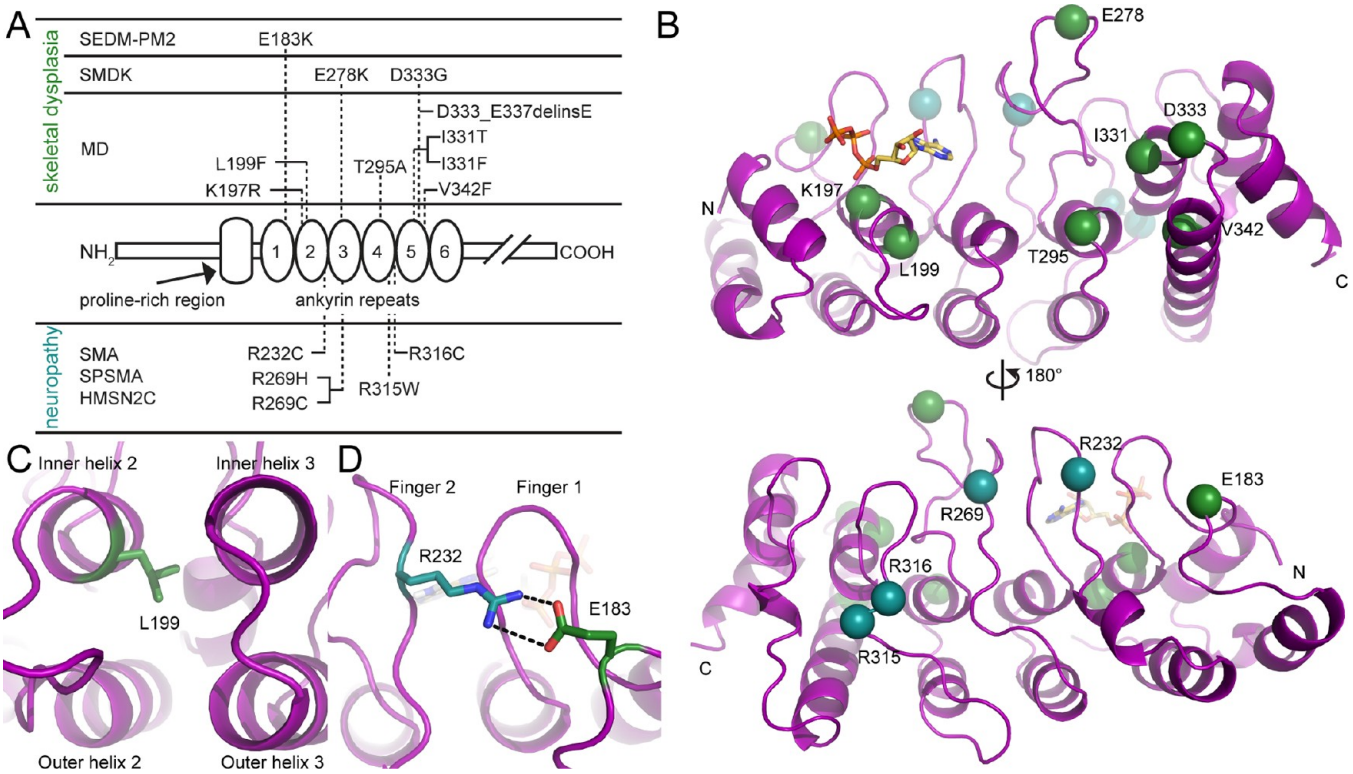

Figure 6. Mutations associated with human diseases in hTRPV4-ARD. (A) Positions of mutations associated with human inherited diseases that lie within hTRPV4-ARD. Abbreviations: SEDM, spondyloepiphyseal dysplasia, type Maroteaux; SMDK, spondylometaphyseal dysplasia, type Kozolowski; MD, metatropic dysplasia; SMA, spinal muscular atrophy; SPMA, scapuloperoneal spinal muscular atrophy; CMTC2, Charcot-Marie-Tooth disease type 2C; HMSN2C, hereditary motor and sensory neuropathy 2C. This figure was inspired by ref 51. (B) Location of the disease-causing mutations within TRPV4-ARD. Shown as spheres are 12 residue positions at which a total of 15 mutations causing human inherited diseases have been identified. The ATP molecule is shown as sticks. Skeletal dysplasia and neurophathy mutations are depicted as green and blue spheres, respectively. (C) Leu199 is located at the hydrophobic interface between ANK2 and ANK3. (D) Glu183 and Arg232 form a salt bridge on the convex face of TRPV4-ARD.

of skeletal dysplasia mutants (35.6 ± 1.6 °C; n = 24) is significantly lower than those of the wild type (37.93 ± 0.08 °C; n = 8; p = 0.0005) and neuropathy mutants (36.9 ± 1.5 °C; n = 15; p = 0.017), although not all mutants obey this trend (Figure 7A).

ATP Binding by hTRPV4-ARD Mutants. Most disease-associated mutations in TRPV4-ARD cause substitutions of surface-exposed side chains. This suggests that interactions with other factors, such as other regions of the TRPV4 protein and/or regulatory ligands, are affected. Because ATP is a known ligand, we tested the ability of the hTRPV4-ARDs with disease-causing mutations to bind ATP using an ATP-agarose pull-down assay (Figure 7B,C). Four mutants, K197R, R232C, R269H, and V342F, showed significantly weakened ATP binding. Lys197, which directly interacts with ATP in our ATP-bound hTRPV4-ARD structure (Figure 3B), showed one of the greatest reductions in the level of ATP binding. This is also consistent with previously published experiments in which corresponding residues Lys183 of cTRPV4-ARD and Lys160 of rTRPV1-ARD were shown to be crucial for ATP binding.[7,8] In contrast, the reduction in the level of ATP binding observed for R232C and R269H is surprising because both residues are on the surface opposite the ATP-binding site (Figure 6B). Similarly, ATP binding is significantly enhanced by the E183K and E278K mutations, although these residues also have no direct interaction with ATP. These results suggest that, although the interaction of ATP is specific to the ATP-binding site observed in our structure,[8] it is influenced by the general

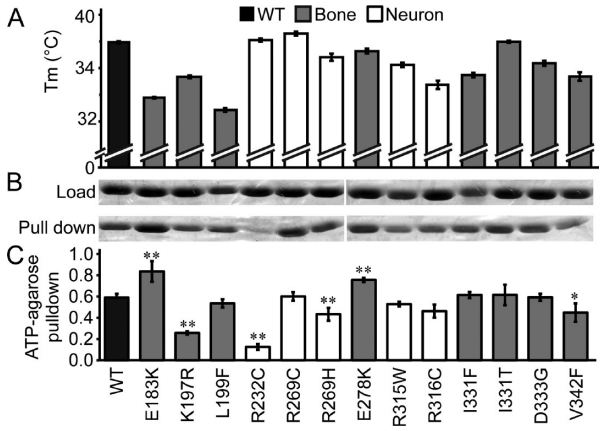

Figure 7. Thermal stability and ATP binding of hTRPV4-ARD mutants associated with inherited diseases. (A) The T_m determined by CD spectrometry in a phosphate-based buffer is plotted for wild-type and mutant hTRPV4-ARDs. The statistical significance is shown in Table S4 of the Supporting Information. (B) Coomassie-stained gels show wild-type and mutant TRPV4-ARDs loaded (top) and bound to ATP-agarose (bottom). (C) Normalized intensity of recovered protein (mean ± SD; n = 3). The statistical significance of the change in binding to ATP-agarose with respect to wild type (WT) was determined by a multiple-comparison test using Dunnett's method, with $p < 0.05$ and $p < 0.01$ indicated by one asterisk and two asterisks, respectively.

dx.doi.org/10.1021/bi300279b | *Biochemistry* 2012, 51, 6195−6206

electrostatic properties of hTRPV4-ARD. Because intracellular ATP sensitizes TRPV4 channel activity,[8] enhanced ATP binding may result in higher channel activity, leading to constitutive basal activity. However, although several mutations either impaired or enhanced ATP binding, there was no correlation between the disease phenotypes and the ATP-binding phenotype.

In summary, enhanced ATP binding in E183K and E278K could contribute to the constitutive TRPV4 activity that is thought to lead to the TRPV4-linked disease phenotypes. However, it is difficult to explain the different disease phenotypes observed, including neuropathy and skeletal dysplasia, on the basis of only changes in thermal stability or ATP binding (Figure 7A,C), suggesting complex and unidentified mechanisms for regulating TRPV4 channel activity in different tissues.

DISCUSSION

In this study, we determined the structures of ATP-free and -bound hTRPV4-ARD and compared them with the structures of other TRPV-ARDs. Structural analyses revealed the flexible Finger 3 as a possible switch for regulating channel activity. Biochemical analyses and MD simulations indicated that ATP contributed to protein stability in TRPV-ARDs possessing ATP binding ability. Finally, a series of biochemical analyses of the disease-associated mutants showed that several have impaired thermal stability and/or ATP binding ability.

The new pair of crystal structures of the ATP-free and -bound forms of TRPV4-ARD revealed minimal conformational changes in the presence of bound ligand. The long and flexible Finger 3 undergoes the largest conformational change. In the process, a patch of aromatic residues is affected, such that a number of these aromatic residues are buried in the presence of ATP. This suggests that a regulatory signal could be exposed or hidden by a Finger 3 conformational change, to affect the sensitization of TRPV4 and the related TRPV1 channel by ATP.[7,8] In other words, ATP binding may control the accessibility of a regulatory surface, which could interact intramolecularly with other parts of the TRPV4 channel or intermolecularly with additional regulatory factors. One candidate for such a regulatory factor is calmodulin, which was shown to require residues within the ATP-binding site for binding to TRPV4-ARD.[8]

It is interesting that the ATP-bound ARD structures of both TRPV1 and TRPV4, with their packed forms of Finger 3, are similar to those of TRPV2 and TRPV6, which lack the ability to bind ATP. Although it does not bind ATP, in phylogenetic analyses TRPV2 clusters with TRPV1, TRPV3, and TRPV4, which can bind ATP. This clustering and the fact that most ATP-binding residues, including two critical lysines, are conserved in TRPV2[8] suggest that TRPV2 may have lost its ATP binding ability in a relatively recent evolutionary process. A previous study attempted to generate a TRPV2-ARD mutant that could bind ATP and/or CaM by introducing two mutations: D78N, which neutralizes a negatively charged side chain in the proximity of the phosphate interaction site, and H165Q, which could restore the adenine-binding pocket.[8] Although neither of the single mutants bound ATP, the D78N/H165Q double mutant bound ATP weakly but significantly, suggesting that additional residues are essential for ATP binding. Our structure of ATP-bound TRPV4-ARD suggests a candidate, Phe231, which is conserved in the rTRPV1-ARD ATP-binding site (Tyr194) but not in TRPV2 and TRPV6 (Figure 3D). Comparing the TRPV-ARD structures suggests that this aromatic residue buttresses the adenine-binding pocket.

Several lines of evidence indicate that ATP binding increases the protein stability of both TRPV1- and TRPV4-ARD (Figures 4 and 5 and Figure S1 of the Supporting Information). Interestingly, TRPV4-ARD showed a T_m near body temperature (37.1 ± 0.1 °C), suggesting that the ARD could be quite sensitive to changes in physiological temperature. In such a situation, a small but significant increase in T_m induced by binding of a ligand such as that observed here for ATP (37.9 ± 0.2 °C) may make a large contribution to protein stability at body temperature. It has been reported that TRPV4 is activated by warm temperatures (threshold for activation of ∼34 °C) and shows basal constitutive activity around body temperature.[13] Furthermore, it has been suggested that some unfolding event may be responsible for the thermosensitivity of TRP channels.[50] Therefore, ARD stabilization by ligand binding may fine-tune TRPV4 function and basal activity levels, although the relationship between the stability of ARD and channel activity remains speculative.

TRPV4 is unusual among the TRPV ion channels because a large number of dominant missense mutations that cause a whole spectrum of human skeletal dysplasias and neurodegenerative diseases have been identified. In particular, the neurodegenerative disease-causing mutations all localize to one surface of the ARD.[49] In contrast, the skeletal dysplasia mutations spread throughout the protein,[51] although a number of them are found in the ARD. We studied a total of 15 mutations at 12 positions localized to the ARD, five neurodegenerative disease mutations and 10 skeletal dysplasia mutations. Recently, two new mutations, Q239H (associated with skeletal dysplasia and located within the adenine pocket of the ATP-binding site) and R316H (associated with CMT2C like the previously identified R316C), have been reported in the ARD.[52,53] Several hTRPV4 mutants, including both neurodegenerative mutations (R232C, R269C, R269H, R315W, and R316C) and skeletal dysplasia mutations (I331F and D333G), cause high basal activity and enhanced response to stimuli when expressed heterologously in HEK293 cells and were inferred to cause cell death because of high Ca^{2+} influx.[26−28,46,53−55] The constitutive activity of hTRPV4 mutants is consistent with their dominant disease phenotypes. However, how different tissue-specific phenotypes are observed when both types of mutations result in a similar cellular phenotype remains unexplained.

We therefore generated 13 of the ARD mutant proteins and compared several of their biochemical properties. We did find several mutations causing significant enhancement or reduction in ARD thermal stability and/or ATP binding. These changes could play a part in the disease mechanisms. Most hTRPV4-ARD mutants showed significantly reduced thermal stability, suggesting that the ARD thermal stability may contribute to the regulation of channel activity. For example, the ARD stability could alter the functional channel population as the N-terminus of TRPV4 has been reported to be important for tetramer assembly.[56] However, a lower T_m does not provide a general correlation to TRPV4 function because R269C, which showed a T_m higher than that of the wild type, has been reported to cause the constitutive activity of the channel.[27,28] Of note, the enhanced ATP binding by two skeletal dysplasia mutations, E183K and E278K, suggests a mechanism for increased TRPV4 activity and Ca^{2+} influx because intracellular ATP has been shown to sensitize TRPV4.[8]

Biochemical analyses in this study suggested two possible mechanisms for how mutations in TRPV4-ARD affect channel activity: reduced ARD thermal stability and enhanced ATP binding. However, it is difficult to explain the disease-specific segregation on the basis of only these two biochemical phenotypes, suggesting that additional mechanisms are likely at play in the regulation of the TRPV4 channel. We also did not see a correlation between thermal stability and ATP binding, suggesting that there is no clear functional relationship between these two phenotypes. Our results therefore leave us with two broad hypotheses. (1) Disease-causing TRPV4 mutations affect diverse regulatory mechanisms, converging to bone or neuron-related phenotypes in how they ultimately affect TRPV4 activity. (2) The most important common mechanisms remain to be identified. That is, there could be regulatory factors or mechanisms specific to each tissue. Further understanding of the mechanisms that cause the human inherited diseases will therefore require the identification of tissue-specific biochemical phenotypes, as well as additional cell biology and electrophysiology studies to link biochemical findings to ion channel function.

■ ASSOCIATED CONTENT

Supporting Information

TRPV-ARD structures used in this study (Table S1), structural similarity between TRPV4-ARD and other TRPV-ARDs (Table S2), molecular dynamics simulations of rat TRPV1-ARD (Table S3), T_m values of wild-type and mutant TRPV4-ARD proteins (Table S4), hTRPV4-ARD cysteine modification assay (Figure S1), stabilities of TRPV1-ARD in equilibrium and SMD simulations (Figure S2), and thermal stabilities of wild-type and mutant TRPV4-ARD proteins (Figure S3). This material is available free of charge via the Internet at http://pubs.acs.org.

■ AUTHOR INFORMATION

Corresponding Author

*Department of Molecular and Cellular Biology, Harvard University, 52 Oxford St., Cambridge, MA 02138. Telephone: (617) 495-5616. Fax: (617) 496-9684. E-mail: gaudet@mcb.harvard.edu.

Present Address

‡Howard Hughes Medical Institute and Department of Biochemistry, University of Washington, Seattle, WA 98195.

Funding

This work was funded by National Institutes of Health Grant R01GM081340 to R.G. This work is based upon research conducted at the Advanced Photon Source on the Northeastern Collaborative Access Team beamlines supported by Grant RR-15301 from the National Center for Research Resources. The Advanced Photon Source is supported by the U.S. Department of Energy, Office of Basic Energy Sciences, under Contract DE-AC02-06CH11357. M.S. was a Howard Hughes Medical Institute Fellow of the Helen Hay Whitney Foundation.

Notes

The authors declare no competing financial interest.

■ ACKNOWLEDGMENTS

We thank David Neau for assistance with data collection, Dr. Wilhelm A. Weihofen for help with data processing, Dr. Charlotte J. Sumner for providing human TRPV4 cDNA, Dr. Ute Hellmich for comments, and current and former lab members for technical help and discussions.

■ ABBREVIATIONS

ANK, ankyrin repeat; ARD, ankyrin repeat domain; CaM, calmodulin; CD, circular dichroism; DTT, dithiothreitol; EDTA, ethylenediaminetetraacetic acid; HEPES, 4-(2-hydroxyethyl)-1-piperazineethanesulfonic acid; IPTG, isopropyl β-D-thiogalactopyranoside; MD, molecular dynamics; PAGE, polyacrylamide gel electrophoresis; PDB, Protein Data Bank; PEG, polyethylene glycol; rmsd, root-mean-square deviation; SDS, sodium dodecyl sulfate; SMD, steered molecular dynamics; TRP, transient receptor potential; TRPV, TRP vanilloid.

■ REFERENCES

(1) Clapham, D. E. (2003) TRP channels as cellular sensors. *Nature 426*, 517−524.

(2) Clapham, D. E., Montell, C., Schultz, G., and Julius, D. (2003) International Union of Pharmacology. XLIII. Compendium of voltage-gated ion channels: Transient receptor potential channels. *Pharmacol. Rev. 55*, 591−596.

(3) Wu, L. J., Sweet, T. B., and Clapham, D. E. (2010) International Union of Basic and Clinical Pharmacology. LXXVI. Current progress in the mammalian TRP ion channel family. *Pharmacol. Rev. 62*, 381−404.

(4) Tominaga, M., and Tominaga, T. (2005) Structure and function of TRPV1. *Pfluegers Arch. 451*, 143−150.

(5) van de Graaf, S. F., Hoenderop, J. G., and Bindels, R. J. (2006) Regulation of TRPV5 and TRPV6 by associated proteins. *Am. J. Physiol. 290*, F1295−F1302.

(6) Rosenbaum, T., Gordon-Shaag, A., Munari, M., and Gordon, S. E. (2004) Ca^{2+}/calmodulin modulates TRPV1 activation by capsaicin. *J. Gen. Physiol. 123*, 53−62.

(7) Lishko, P. V., Procko, E., Jin, X., Phelps, C. B., and Gaudet, R. (2007) The ankyrin repeats of TRPV1 bind multiple ligands and modulate channel sensitivity. *Neuron 54*, 905−918.

(8) Phelps, C. B., Wang, R. R., Choo, S. S., and Gaudet, R. (2010) Differential regulation of TRPV1, TRPV3, and TRPV4 sensitivity through a conserved binding site on the ankyrin repeat domain. *J. Biol. Chem. 285*, 731−740.

(9) Prescott, E. D., and Julius, D. (2003) A modular PIP2 binding site as a determinant of capsaicin receptor sensitivity. *Science 300*, 1284−1288.

(10) Ufret-Vincenty, C. A., Klein, R. M., Hua, L., Angueyra, J., and Gordon, S. E. (2011) Localization of the PIP2 sensor of TRPV1 ion channels. *J. Biol. Chem. 286*, 9688−9698.

(11) Numazaki, M., Tominaga, T., Takeuchi, K., Murayama, N., Toyooka, H., and Tominaga, M. (2003) Structural determinant of TRPV1 desensitization interacts with calmodulin. *Proc. Natl. Acad. Sci. U.S.A. 100*, 8002−8006.

(12) Liedtke, W., Choe, Y., Marti-Renom, M. A., Bell, A. M., Denis, C. S., Sali, A., Hudspeth, A. J., Friedman, J. M., and Heller, S. (2000) Vanilloid receptor-related osmotically activated channel (VR-OAC), a candidate vertebrate osmoreceptor. *Cell 103*, 525−535.

(13) Guler, A. D., Lee, H., Iida, T., Shimizu, I., Tominaga, M., and Caterina, M. (2002) Heat-evoked activation of the ion channel, TRPV4. *J. Neurosci. 22*, 6408−6414.

(14) Watanabe, H., Vriens, J., Suh, S. H., Benham, C. D., Droogmans, G., and Nilius, B. (2002) Heat-evoked activation of TRPV4 channels in a HEK293 cell expression system and in native mouse aorta endothelial cells. *J. Biol. Chem. 277*, 47044−47051.

(15) Watanabe, H., Vriens, J., Prenen, J., Droogmans, G., Voets, T., and Nilius, B. (2003) Anandamide and arachidonic acid use epoxyeicosatrienoic acids to activate TRPV4 channels. *Nature 424*, 434−438.

(16) Liedtke, W. (2005) TRPV4 as osmosensor: A transgenic approach. *Pfluegers Arch. 451*, 176−180.

(17) Tominaga, M., and Caterina, M. J. (2004) Thermosensation and pain. *J. Neurobiol. 61*, 3−12.

(18) Mochizuki, T., Sokabe, T., Araki, I., Fujishita, K., Shibasaki, K., Uchida, K., Naruse, K., Koizumi, S., Takeda, M., and Tominaga, M. (2009) The TRPV4 cation channel mediates stretch-evoked Ca^{2+} influx and ATP release in primary urothelial cell cultures. *J. Biol. Chem. 284*, 21257−21264.
(19) Sokabe, T., and Tominaga, M. (2010) The TRPV4 cation channel: A molecule linking skin temperature and barrier function. *Commun. Integr. Biol. 3*, 619−621.
(20) Shibasaki, K., Suzuki, M., Mizuno, A., and Tominaga, M. (2007) Effects of body temperature on neural activity in the hippocampus: Regulation of resting membrane potentials by transient receptor potential vanilloid 4. *J. Neurosci. 27*, 1566−1575.
(21) Alessandri-Haber, N., Dina, O. A., Joseph, E. K., Reichling, D., and Levine, J. D. (2006) A transient receptor potential vanilloid 4-dependent mechanism of hyperalgesia is engaged by concerted action of inflammatory mediators. *J. Neurosci. 26*, 3864−3874.
(22) Masuyama, R., Vriens, J., Voets, T., Karashima, Y., Owsianik, G., Vennekens, R., Lieben, L., Torrekens, S., Moermans, K., Vanden Bosch, A., Bouillon, R., Nilius, B., and Carmeliet, G. (2008) TRPV4-mediated calcium influx regulates terminal differentiation of osteoclasts. *Cell Metab. 8*, 257−265.
(23) Nilius, B., and Owsianik, G. (2010) Transient receptor potential channelopathies. *Pfluegers Arch. 460*, 437−450.
(24) Verma, P., Kumar, A., and Goswami, C. (2010) TRPV4-mediated channelopathies. *Channels 4*, 319−328.
(25) Rock, M. J., Prenen, J., Funari, V. A., Funari, T. L., Merriman, B., Nelson, S. F., Lachman, R. S., Wilcox, W. R., Reyno, S., Quadrelli, R., Vaglio, A., Owsianik, G., Janssens, A., Voets, T., Ikegawa, S., Nagai, T., Rimoin, D. L., Nilius, B., and Cohn, D. H. (2008) Gain-of-function mutations in TRPV4 cause autosomal dominant brachyolmia. *Nat. Genet. 40*, 999−1003.
(26) Krakow, D., Vriens, J., Camacho, N., Luong, P., Deixler, H., Funari, T. L., Bacino, C. A., Irons, M. B., Holm, I. A., Sadler, L., Okenfuss, E. B., Janssens, A., Voets, T., Rimoin, D. L., Lachman, R. S., Nilius, B., and Cohn, D. H. (2009) Mutations in the gene encoding the calcium-permeable ion channel TRPV4 produce spondylometaphyseal dysplasia, Kozlowski type and metatropic dysplasia. *Am. J. Hum. Genet. 84*, 307−315.
(27) Deng, H. X., Klein, C. J., Yan, J., Shi, Y., Wu, Y., Fecto, F., Yau, H. J., Yang, Y., Zhai, H., Siddique, N., Hedley-Whyte, E. T., Delong, R., Martina, M., Dyck, P. J., and Siddique, T. (2010) Scapuloperoneal spinal muscular atrophy and CMT2C are allelic disorders caused by alterations in TRPV4. *Nat. Genet. 42*, 165−169.
(28) Landoure, G., Zdebik, A. A., Martinez, T. L., Burnett, B. G., Stanescu, H. C., Inada, H., Shi, Y., Taye, A. A., Kong, L., Munns, C. H., Choo, S. S., Phelps, C. B., Paudel, R., Houlden, H., Ludlow, C. L., Caterina, M. J., Gaudet, R., Kleta, R., Fischbeck, K. H., and Sumner, C. J. (2010) Mutations in TRPV4 cause Charcot-Marie-Tooth disease type 2C. *Nat. Genet. 42*, 170−174.
(29) Jin, X., Touhey, J., and Gaudet, R. (2006) Structure of the N-terminal ankyrin repeat domain of the TRPV2 ion channel. *J. Biol. Chem. 281*, 25006−25010.
(30) Otwinowski, Z., and Minor, W. (1997) Processing of X-ray Diffraction Data Collected in Oscillation Mode. *Methods Enzymol. 276*, 307−326.
(31) Vagin, A., and Teplyakov, A. (2000) An approach to multi-copy search in molecular replacement. *Acta Crystallogr. D56*, 1622−1624.
(32) McCoy, A. J., Grosse-Kunstleve, R. W., Adams, P. D., Winn, M. D., Storoni, L. C., and Read, R. J. (2007) Phaser crystallographic software. *J. Appl. Crystallogr. 40*, 658−674.
(33) Emsley, P., and Cowtan, K. (2004) Coot: Model-building tools for molecular graphics. *Acta Crystallogr. D60*, 2126−2132.
(34) Murshudov, G. N., Vagin, A. A., and Dodson, E. J. (1997) Refinement of macromolecular structures by the maximum-likelihood method. *Acta Crystallogr. D53*, 240−255.
(35) Humphrey, W., Dalke, A., and Schulten, K. (1996) VMD: Visual molecular dynamics. *J. Mol. Graphics 14*, 27−38.
(36) Phillips, J. C., Braun, R., Wang, W., Gumbart, J., Tajkhorshid, E., Villa, E., Chipot, C., Skeel, R. D., Kale, L., and Schulten, K. (2005) Scalable molecular dynamics with NAM. *J. Comput. Chem. 26*, 1781−1802.
(37) MacKerell, A. D., Jr., Bashford, D., Bellott, M., Dunbrack, R. L., Jr., Evanseck, J. D., Field, M. J., Fischer, S., Gao, J., Guo, H., Ha, S., Joseph-McCarthy, D., Kuchnir, L., Kuczera, K., Lau, F. T. K., Mattos, C., Michnick, S., Ngo, T., Nguyen, D. T., Prodhom, B., Reiher, W. E., III, Roux, B., Schlenkrich, M., Smith, J. C., Stote, R., Straub, J., Watanabe, M., Wiórkiewicz-Kuczera, J., Yin, D., and Karplus, M. (1998) All-Atom Empirical Potential for Molecular Modeling and Dynamics Studies of Proteins. *J. Phys. Chem. B 102*, 3586−3616.
(38) Mackerell, A. D., Jr., Feig, M., and Brooks, C. L., III (2004) Extending the treatment of backbone energetics in protein force fields: Limitations of gas-phase quantum mechanics in reproducing protein conformational distributions in molecular dynamics simulations. *J. Comput. Chem. 25*, 1400−1415.
(39) McCleverty, C. J., Koesema, E., Patapoutian, A., Lesley, S. A., and Kreusch, A. (2006) Crystal structure of the human TRPV2 channel ankyrin repeat domain. *Protein Sci. 15*, 2201−2206.
(40) Phelps, C. B., Huang, R. J., Lishko, P. V., Wang, R. R., and Gaudet, R. (2008) Structural analyses of the ankyrin repeat domain of TRPV6 and related TRPV ion channels. *Biochemistry 47*, 2476−2484.
(41) Croy, C. H., Bergqvist, S., Huxford, T., Ghosh, G., and Komives, E. A. (2004) Biophysical characterization of the free IκBα ankyrin repeat domain in solution. *Protein Sci. 13*, 1767−1777.
(42) Truhlar, S. M., Torpey, J. W., and Komives, E. A. (2006) Regions of IκBα that are critical for its inhibition of NF-κB·DNA interaction fold upon binding to NF-κB. *Proc. Natl. Acad. Sci. U.S.A. 103*, 18951−18956.
(43) Barrick, D., Ferreiro, D. U., and Komives, E. A. (2008) Folding landscapes of ankyrin repeat proteins: Experiments meet theory. *Curr. Opin. Struct. Biol. 18*, 27−34.
(44) Salazar, H., Llorente, I., Jara-Oseguera, A., Garcia-Villegas, R., Munari, M., Gordon, S. E., Islas, L. D., and Rosenbaum, T. (2008) A single N-terminal cysteine in TRPV1 determines activation by pungent compounds from onion and garlic. *Nat. Neurosci. 11*, 255−261.
(45) Isralewitz, B., Gao, M., and Schulten, K. (2001) Steered molecular dynamics and mechanical functions of proteins. *Curr. Opin. Struct. Biol. 11*, 224−230.
(46) Camacho, N., Krakow, D., Johnykutty, S., Katzman, P. J., Pepkowitz, S., Vriens, J., Nilius, B., Boyce, B. F., and Cohn, D. H. (2010) Dominant TRPV4 mutations in nonlethal and lethal metatropic dysplasia. *Am. J. Med. Genet., Part A 152A*, 1169−1177.
(47) Dai, J., Kim, O. H., Cho, T. J., Schmidt-Rimpler, M., Tonoki, H., Takikawa, K., Haga, N., Miyoshi, K., Kitoh, H., Yoo, W. J., Choi, I. H., Song, H. R., Jin, D. K., Kim, H. T., Kamasaki, H., Bianchi, P., Grigelioniene, G., Nampoothiri, S., Minagawa, M., Miyagawa, S. I., Fukao, T., Marcelis, C., Jansweijer, M. C., Hennekam, R. C., Bedeschi, F., Mustonen, A., Jiang, Q., Ohashi, H., Furuichi, T., Unger, S., Zabel, B., Lausch, E., Superti-Furga, A., Nishimura, G., and Ikegawa, S. (2010) Novel and recurrent TRPV4 mutations and their association with distinct phenotypes within the TRPV4 dysplasia family. *J. Med. Genet. 47*, 704−709.
(48) Nishimura, G., Dai, J., Lausch, E., Unger, S., Megarbane, A., Kitoh, H., Kim, O. H., Cho, T. J., Bedeschi, F., Benedicenti, F., Mendoza-Londono, R., Silengo, M., Schmidt-Rimpler, M., Spranger, J., Zabel, B., Ikegawa, S., and Superti-Furga, A. (2010) Spondylo-epiphyseal dysplasia, Maroteaux type (pseudo-Morquio syndrome type 2), and parastremmatic dysplasia are caused by TRPV4 mutations. *Am. J. Med. Genet., Part A 152A*, 1443−1449.
(49) Zimon, M., Baets, J., Auer-Grumbach, M., Berciano, J., Garcia, A., Lopez-Laso, E., Merlini, L., Hilton-Jones, D., McEntagart, M., Crosby, A. H., Barisic, N., Boltshauser, E., Shaw, C. E., Landoure, G., Ludlow, C. L., Gaudet, R., Houlden, H., Reilly, M. M., Fischbeck, K. H., Sumner, C. J., Timmerman, V., Jordanova, A., and Jonghe, P. D. (2010) Dominant mutations in the cation channel gene transient receptor potential vanilloid 4 cause an unusual spectrum of neuropathies. *Brain 133*, 1798−1809.
(50) Clapham, D. E., and Miller, C. (2011) A thermodynamic framework for understanding temperature sensing by transient

receptor potential (TRP) channels. *Proc. Natl. Acad. Sci. U.S.A. 108*, 19492−19497.
(51) Dai, J., Cho, T. J., Unger, S., Lausch, E., Nishimura, G., Kim, O. H., Superti-Furga, A., and Ikegawa, S. (2010) TRPV4-pathy, a novel channelopathy affecting diverse systems. *J. Hum. Genet. 55*, 400−402.
(52) Andreucci, E., Aftimos, S., Alcausin, M., Haan, E., Hunter, W., Kannu, P., Kerr, B., McGillivray, G., Gardner, R. M., Patricelli, M. G., Sillence, D., Thompson, E., Zacharin, M., Zankl, A., Lamande, S. R., and Savarirayan, R. (2011) TRPV4 related skeletal dysplasias: A phenotypic spectrum highlighted byclinical, radiographic, and molecular studies in 21 new families. *Orphanet. J. Rare Dis. 6*, 37.
(53) Klein, C. J., Shi, Y., Fecto, F., Donaghy, M., Nicholson, G., McEntagart, M. E., Crosby, A. H., Wu, Y., Lou, H., McEvoy, K. M., Siddique, T., Deng, H. X., and Dyck, P. J. (2011) TRPV4 mutations and cytotoxic hypercalcemia in axonal Charcot-Marie-Tooth neuropathies. *Neurology 76*, 887−894.
(54) Fecto, F., Shi, Y., Huda, R., Martina, M., Siddique, T., and Deng, H. X. (2011) Mutant TRPV4-mediated toxicity is linked to increased constitutive function in axonal neuropathies. *J. Biol. Chem. 286*, 17281−17291.
(55) Loukin, S., Su, Z., and Kung, C. (2011) Increased basal activity is a key determinant in the severity of human skeletal dysplasia caused by TRPV4 mutations. *PLoS One 6*, e19533.
(56) Schaefer, M. (2005) Homo- and heteromeric assembly of TRP channel subunits. *Pfluegers Arch. 451*, 35−42.